



# Optical Characterization of a GaN-based LED Grown on Patterned Sapphire Substrate

Hui-Yu Cheng<sup>1</sup>, Wei-Liang Chen<sup>1</sup>, Heng Li<sup>2</sup>, Yi-Hsin Huang<sup>1</sup>, Tien-Chang Lu<sup>2</sup>, and Yu-Ming Chang<sup>1\*</sup>

<sup>1</sup> Center for Condensed Matter Sciences, National Taiwan University, 10617, Taipei, Taiwan

<sup>2</sup> Department of Photonics, National Chiao Tung University, Hsinchu, Taiwan

\*Corresponding author: ymchang@ntu.edu.tw

## Abstract

We performed depth-resolved Raman spectral mapping, low temperature photoluminescence (PL) spectral mapping and time-domain fluorescence lifetime Imaging (FLIM) of a GaN-based LED structure grown on a patterned sapphire substrate (PSS). The Raman spectral mapping revealed the stress distribution originating from the PSS and propagating to the MQWs layer near the LED surface. The PL spectral mapping at 77 K revealed several additional peak features, besides the two main peak features associated with the indium concentration in the two different multiple quantum wells of the LED structure. By performing multiple peak fitting analysis, we find that the peak wavelength and intensity distributions are closely associated with the PSS. Furthermore, spatial variations in the PL spectra can be associated with the indium fluctuation distribution induced by strain propagation from the PSS [1]. FLIM measurements provided further evidence for the reduced emission intensities observed in areas of high strain and low indium concentration.

## Fabrication of GaN-based LED

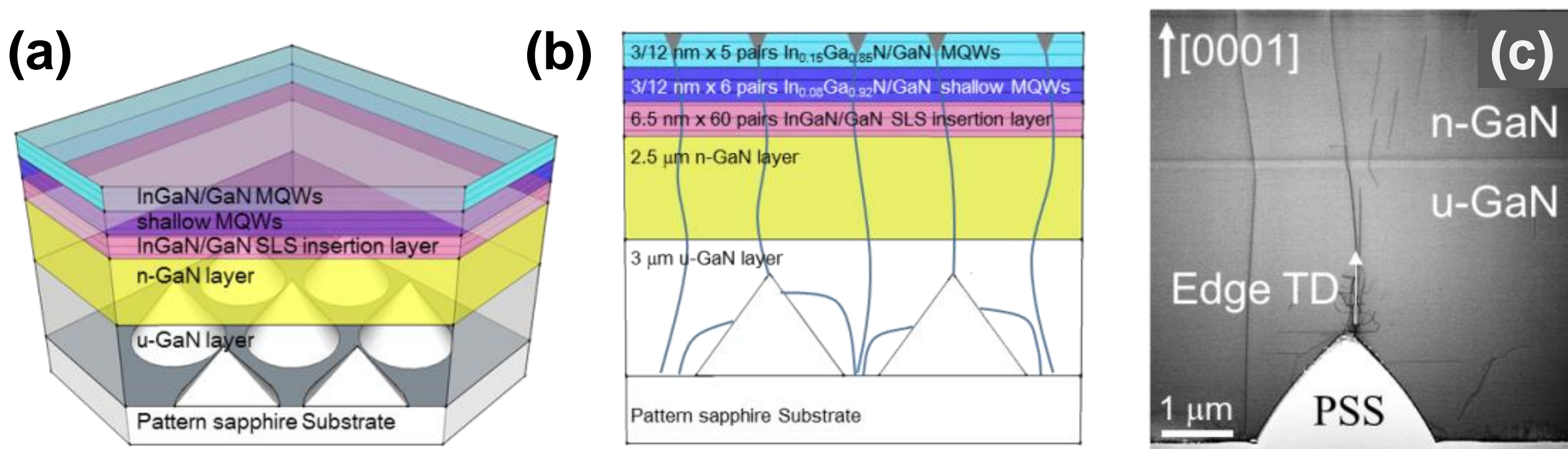


Figure 1. (a) Three-dimension schematic and (b) two-dimensional cross-section schematic of the epitaxial GaN layers grown on PSS, showing the thickness of each layer. The solid blue lines indicate the propagation of threading dislocations, which end up with V-shaped pits on the surface. (c) TEM cross-section image of epitaxial GaN layers around a PSS cone. The LED structure used in this work was grown on a c-plane PSS by metal organic chemical vapor deposition (MOCVD). The final layer consists of an InGaN/GaN multi-quantum wells (MQWs) active layer. There are two groups of quantum wells, each with a different indium composition. The p-GaN layer was not grown in order to investigate the spatial properties of MQWs.

## Raman Spectral Mapping

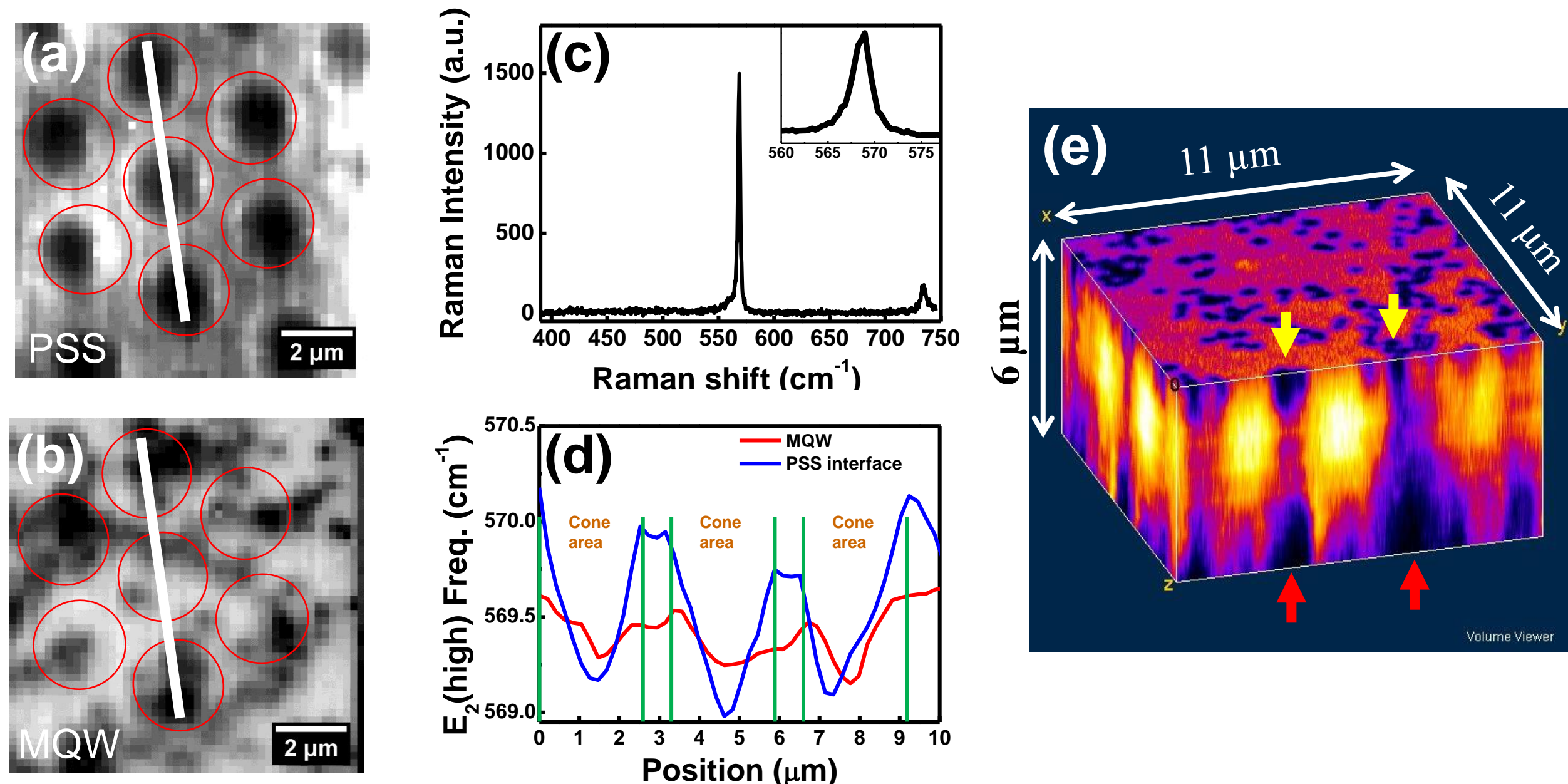


Figure 2. The mapping of GaN  $E_2(\text{high})$  phonon peak intensity at (a) PSS-GaN interface and (b) InGaN/GaN MQWs layer. (c) A typical Raman spectrum collected for the mapping results of (a) and (b). Inset shows a zoom-in view of the  $E_2(\text{high})$  peak. (d) Plot of  $E_2(\text{high})$  phonon peak position variation along the white lines indicated in (a) and (b). The peak position change shows stress variation are correlated with PSS pattern. The PSS cone areas are marked for reference. (e) 3D mapping of  $E_2(\text{high})$  phonon peak intensity in a volume of  $11 \mu\text{m}$  (L)  $\times$   $11 \mu\text{m}$  (W)  $\times$   $6 \mu\text{m}$  (H). The red and yellow arrows mark the positions of the PSS cones and the V-shaped pits, respectively.

## MQW PL Spectra at 77 K

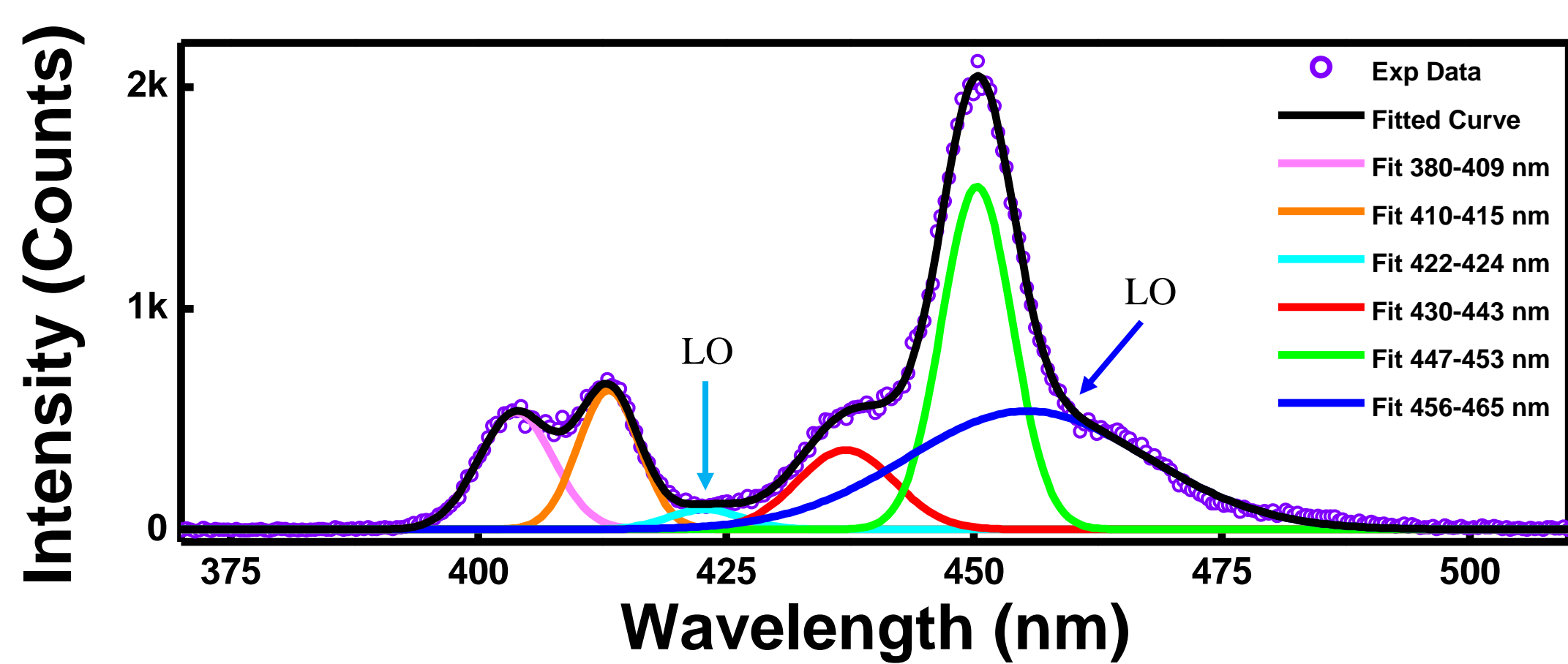


Figure 3. Figure shows a sample spectrum of GaN-based LED at 77 K. The PL emission spectrum can be well fitted by six Gaussian peaks. The wavelength of the two major PL peaks ( $\sim 413$ ,  $\sim 450$  nm) correspond to the dominant PL emission wavelengths of the two  $\text{In}_x\text{Ga}_{1-x}\text{N}$  quantum well groups with designed indium composition (i.e.  $x = 0.08$  and  $0.15$ ). The two blue-shifted minor PL peaks ( $\sim 404$ ,  $\sim 437$  nm) comes from the variation of indium composition. In addition, the two broad features on the low energy shoulder of the main peak are LO phonon-replica transitions.

## Reference

[1] Heng Li, Hui-Yu Cheng, Wei-Liang Chen, *et al.*, *Scientific Reports*, Vol 7, srep 45519, 2017.

## PL Spectral Mapping at 77 K and 293 K

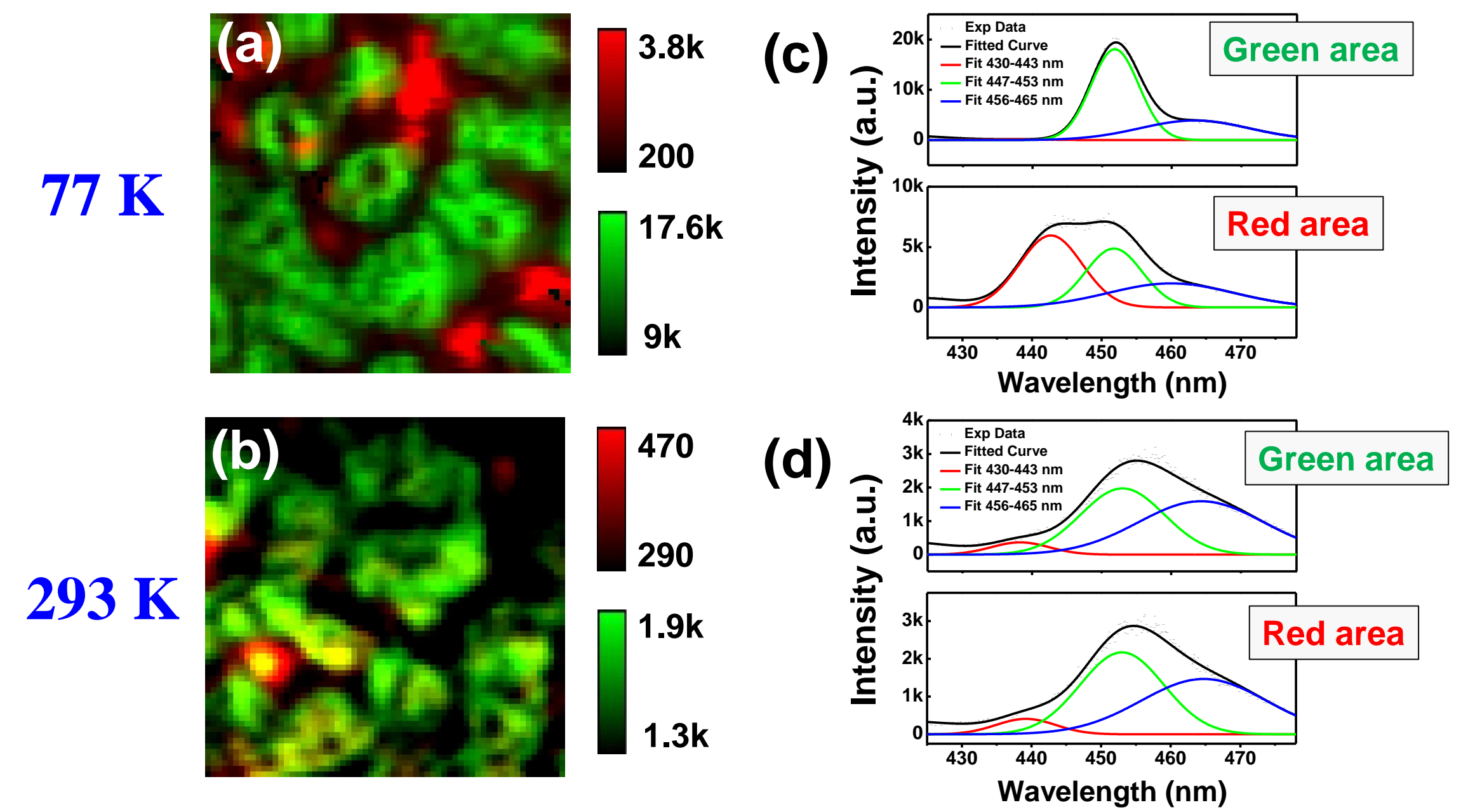


Figure 4. The color mapping of the major and minor PL peaks derived from the curve fitting result of the PL spectral mapping at (a) 77 K and (b) 293 K. The green represents the intensity of the major peaks. (c) and (d) show selected PL spectra representative of the green and red areas shown in (a) and (b). The replica peak appeared in the same areas as the major peaks. The PL components becomes more distinct at low temperature, particularly for the phono-replica component. In the red area PL spectra intensities are low, and minor PL peaks are more blue-shifted. The PL peak intensity pattern shown in (a) strongly suggests the spatial variation of indium composition in the designed  $\text{In}_x\text{Ga}_{1-x}\text{N}$  quantum well groups can be directly related to the PSS-induced residual strain distribution in the MQW layer as shown in Fig. 2(b). The smaller strain for the green area (area above cone), and the larger strain for the red area (area above the flat areas of PSS) can also be seen in the variation of the  $E_2(\text{high})$  peak position shown in Fig. 1(d). The InGaN/GaN MQWs above the cone area exhibit longer emission wavelength, brighter PL emission intensity, smaller residual strain and higher indium composition.

## Fluorescence Lifetime Imaging

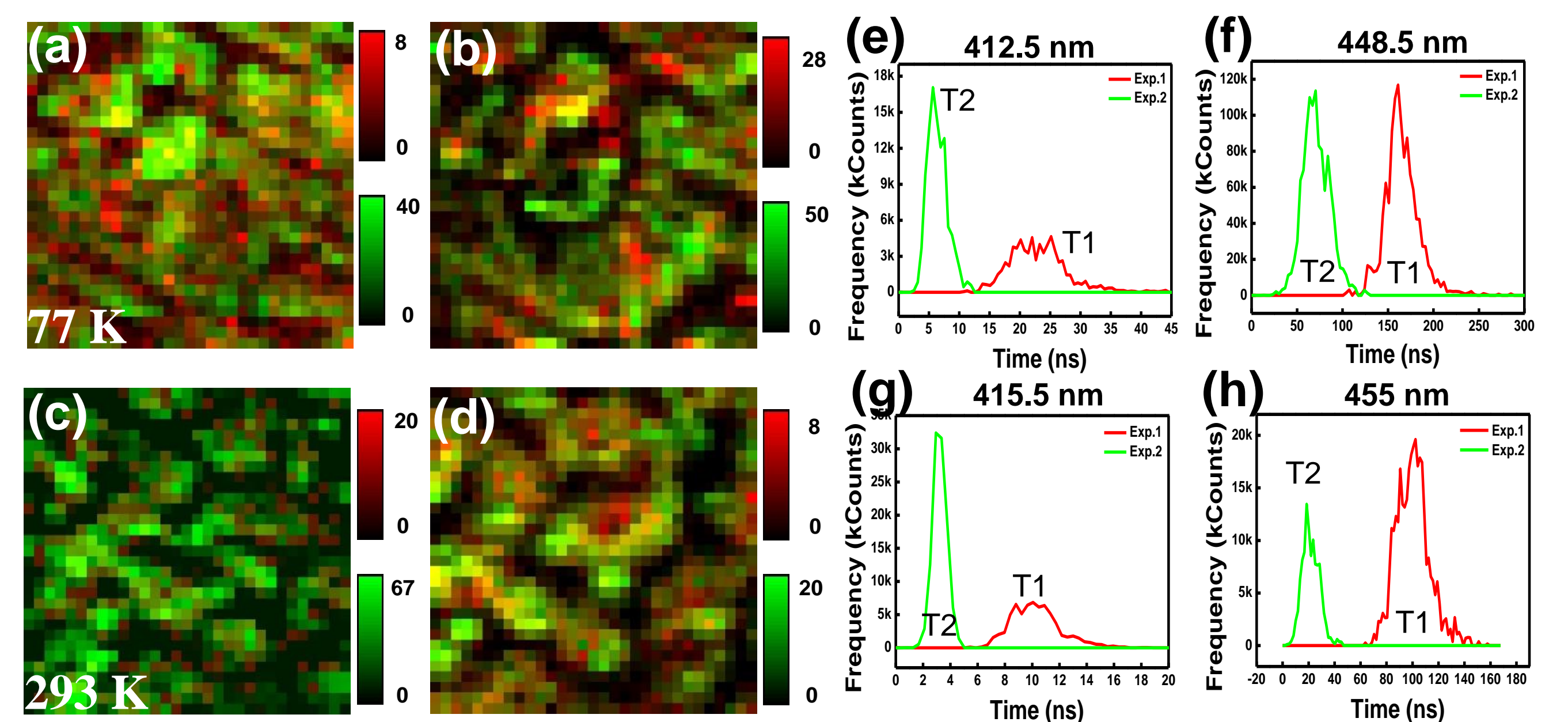


Figure 5. The color mapping of the two fitted lifetimes (T1: red, T2: green) at (a) 412.5 and (b) 448.5 nm PL peak for 77 K, and similar maps at (c) 415.5 and (d) 455 nm PL peak for 293 K. The fitted lifetime distribution of GaN-based LED at indicated wavelength for (e, f) 77 K and (g, h) 293 K.

## Conclusion

The 3D strain distribution and PL emission property of GaN-based LED were measured systematically. We find that the Raman and PL mapping are both correlated with the 3D strain distribution that originated from the PSS-GaN heterointerface. The correlations are summarized in the table below.

MQW PSS	Residual Strain	Emission wavelength	Emission Intensity	Indium Composition	Lifetime Distribution
Cone area	Small	Longer	Bright	Higher	Strong
Flat area	Large	Shorter	Dark	Low	Weak

## Acknowledgement

The authors would like to thank the Ministry of Science and Technology of Taiwan for financial support of this research under Grant No. MOST 105-2119-M-002-046-MY3